Supplement of Atmos. Chem. Phys., 22, 1575–1600, 2022
https://doi.org/10.5194/acp-22-1575-2022-supplement

Atmospheric Chemistry and Physics
Open Access

Supplement of

Weakening of Antarctic stratospheric planetary wave activities in early austral spring since the early 2000s: a response to sea surface temperature trends

Yihang Hu et al.

Correspondence to: Wenshou Tian (wstian@lzu.edu.cn)

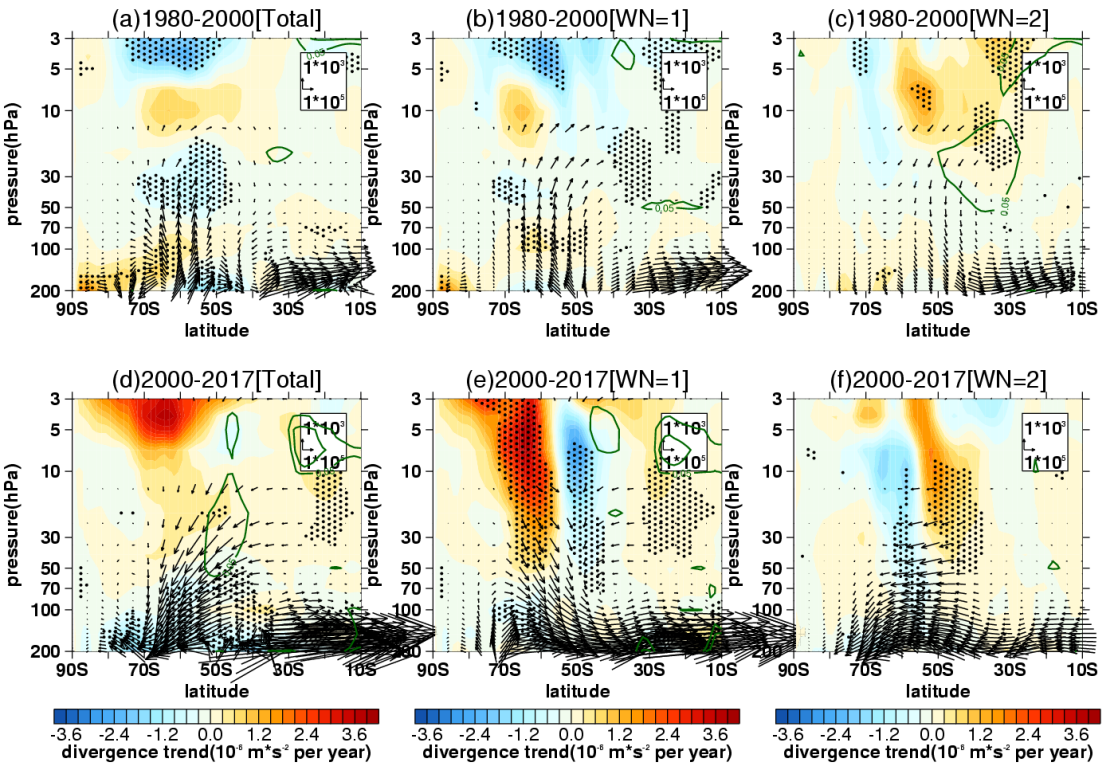

1

2 **FIG. S1.** Same as Fig. 1, except for the August.

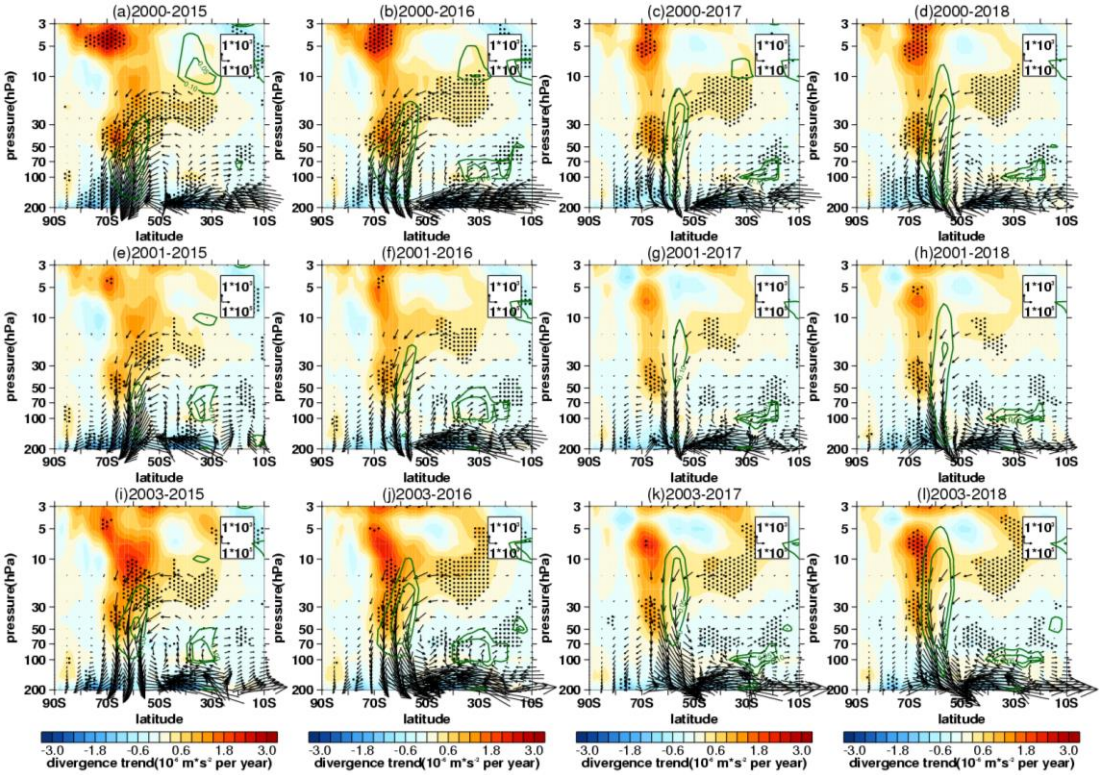

3

4 **FIG. S2.** Trends of Southern Hemispheric undecomposed stratospheric E-P flux

5 (arrows, units in horizontal and vertical components are 10^5 and 10^3 kg·s^{-2} per year,

respectively) and its divergence (shadings) in September over different periods (titles) derived from MERRA-2 dataset. Data in 2002 are removed when calculating trends with beginning year before it. The stippled regions and green contours are the same as Figure 1.

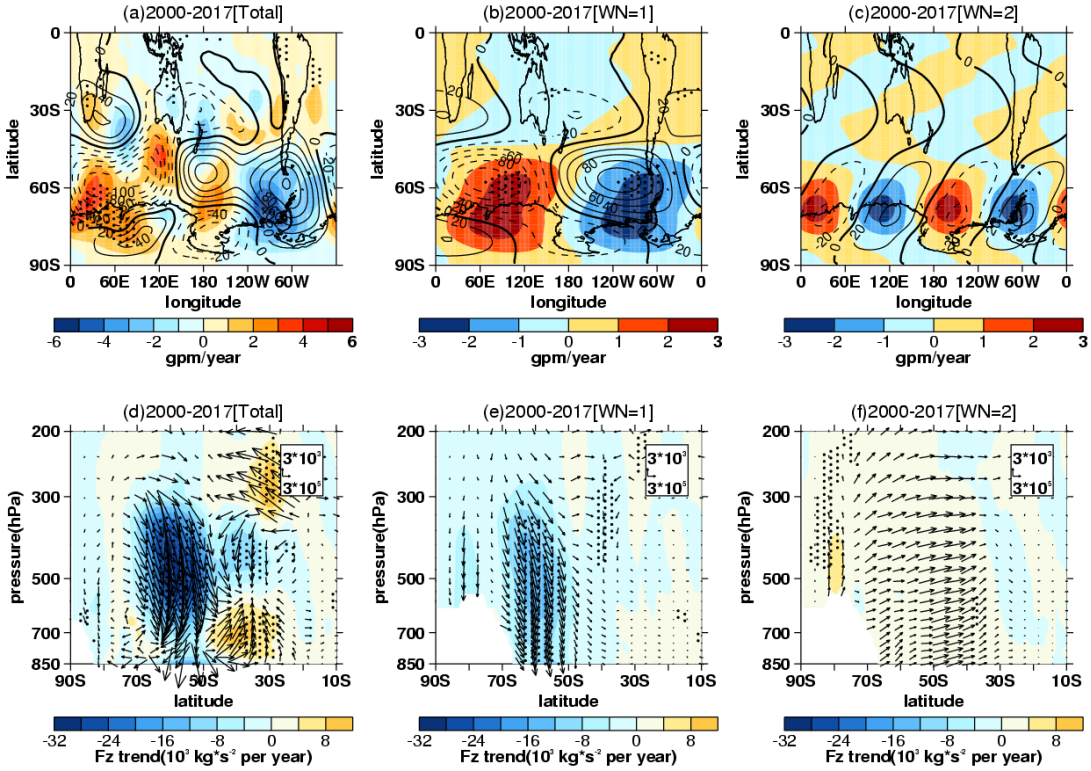

FIG. S3. Same as Fig. 3, except that the values in 2002 are removed.

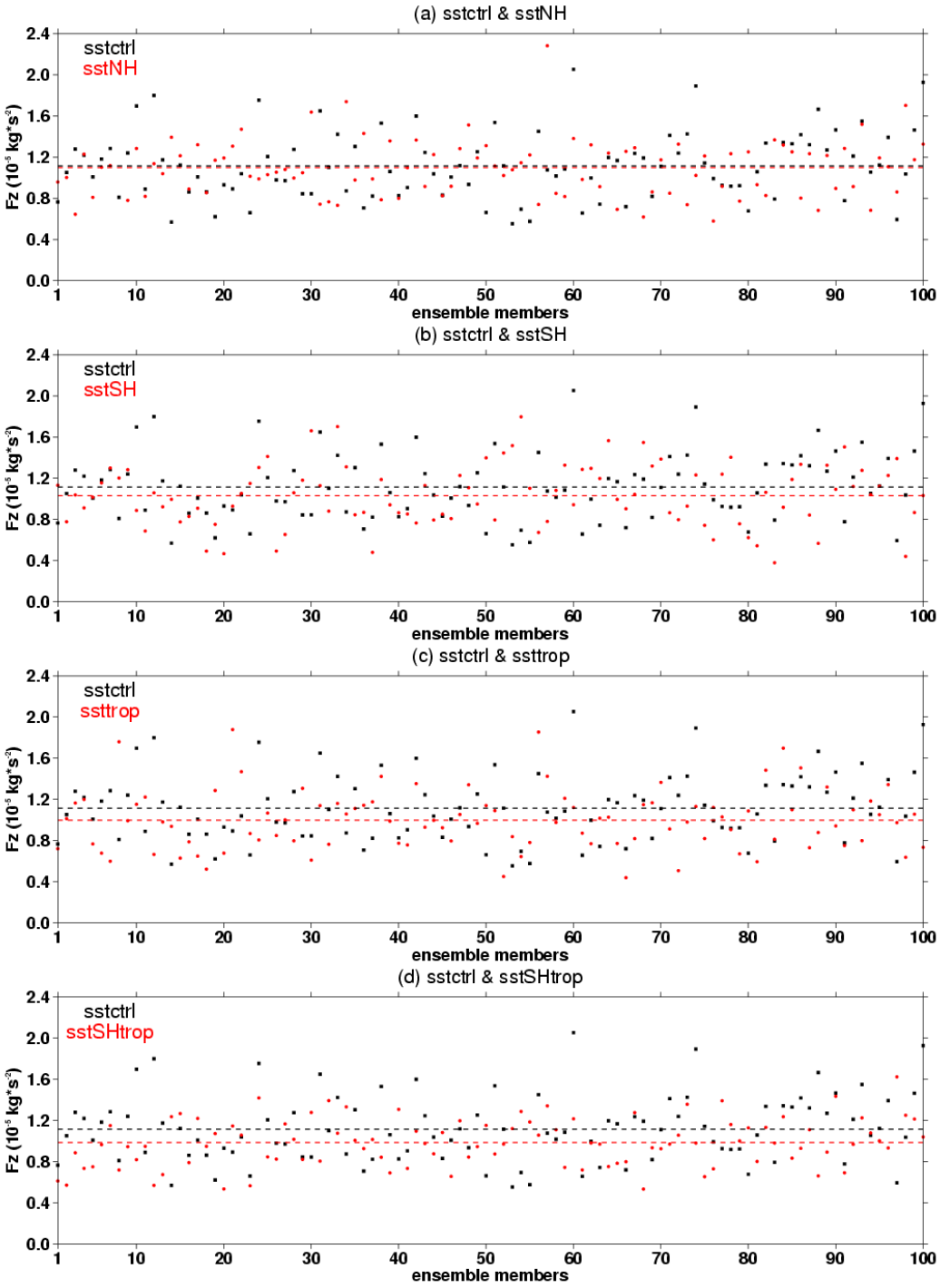

12

13 **FIG. S4.** Stratospheric vertical E-P flux (Fz, area-weighted from 200 hPa to 10 hPa

14 over 70°S-50°S) derived from each ensemble member of control experiment (black

15 squares) and different sensitive experiment (red circles; (a) sstNH; (b) sstSH; (c) ssttrop;

16 (d) sstSHtrop). Black and red horizontal dashed lines represent the ensemble means

17 derived from control experiment and sensitive experiments, respectively.

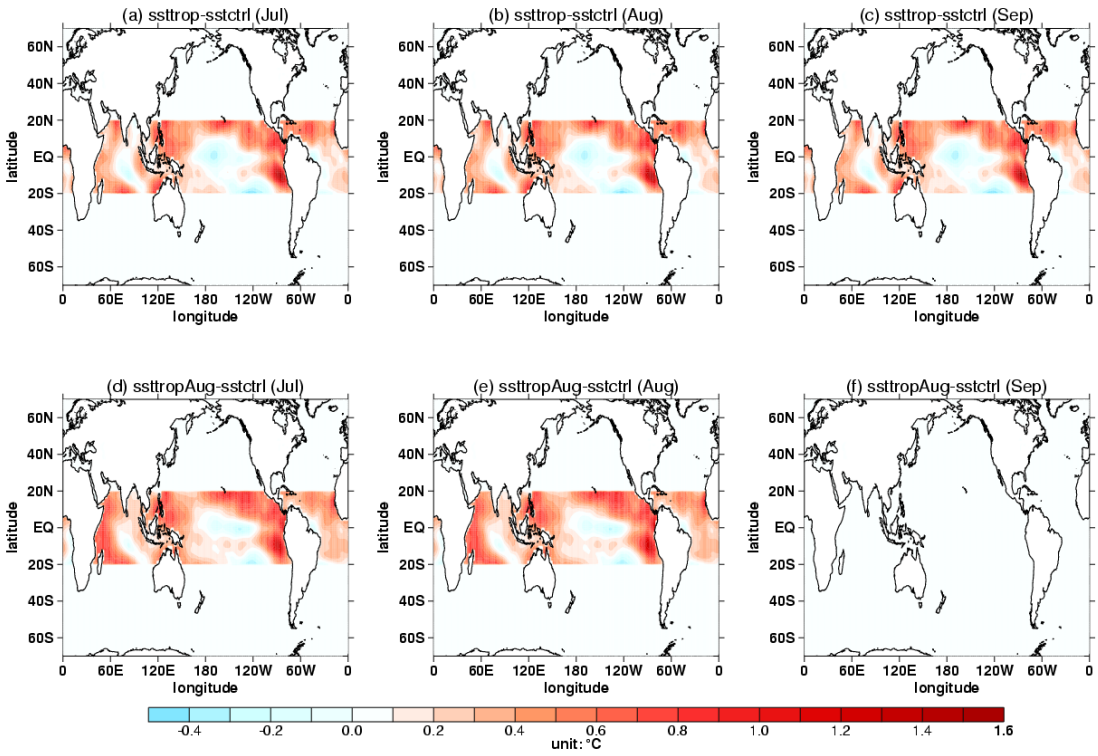

18

19 **FIG. S5.** Differences of SST forcing fields in July (a, d), August (b, e) and September

20 (c, f) between the sensitive experiments ((a, b, c) ssttrop; (d, e, f) ssttropAug) and the

21 control experiment (sstctrl).

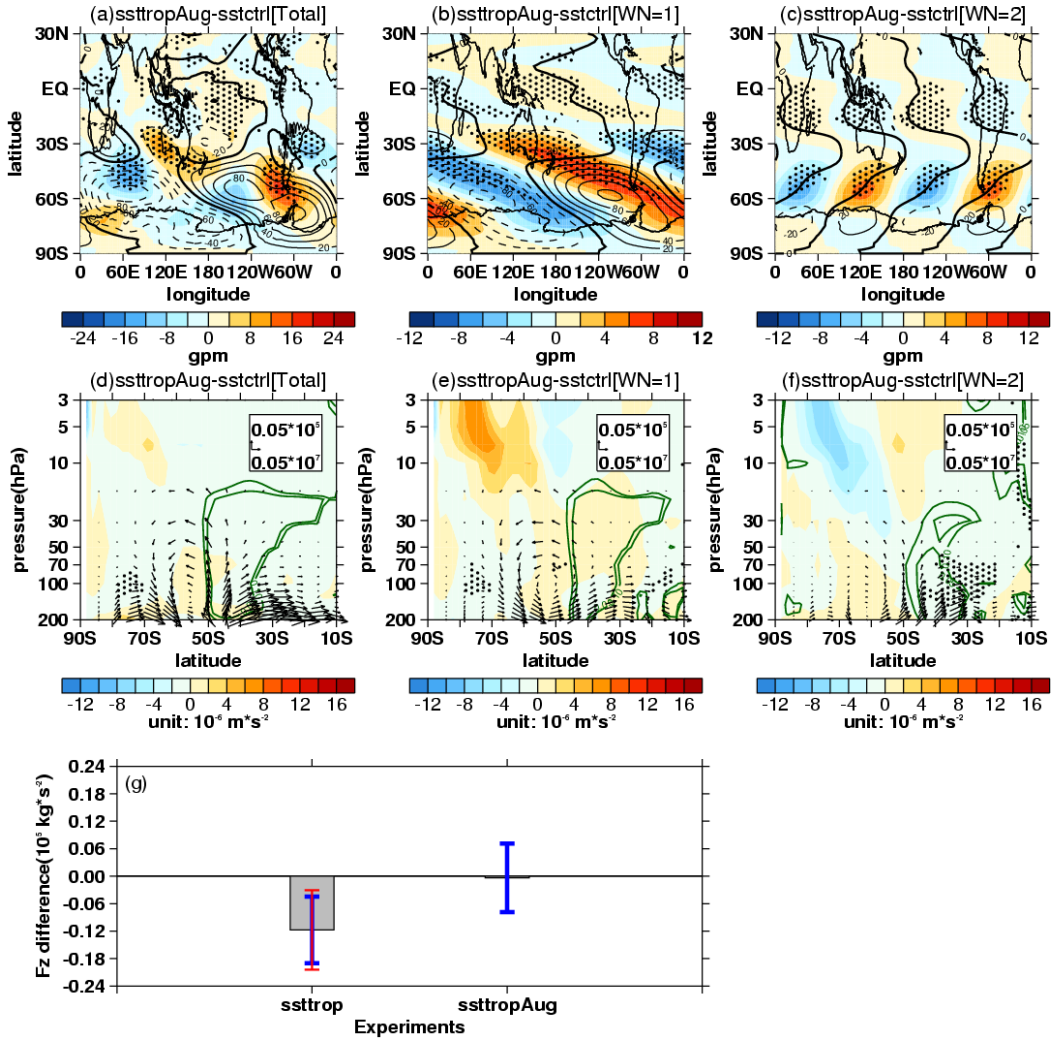

FIG. S6. (a-c) The responses of tropospheric wave sources in experiment ssttropAug: differences of (a) 500 hPa geopotential height zonal deviations with their (b) wave-1 component and (c) wave-2 component between ssttropAug and sstctrl. The mean distributions (contours with an interval of 20 gpm, positive and negative values are depicted by solid and dashed lines, respectively, zeros are depicted by thick solid lines) of them are derived from sstctrl. (d-f) The responses of stratospheric wave activities in experiment ssttropAug: differences of (d) stratospheric E-P flux (arrows, units in horizontal and vertical components are 0.05×10^7 and 0.05×10^5 kg·s^{-2}, respectively) and its divergence (shadings) with their (e) wave-1 component and (f) wave-2 component

between ssttropAug and sstctrl. The stippled regions in Figs. S6a-f represent the mean difference significant at/above the 90% confidence level. The green contours from outside to inside (corresponding to p=0.1 and 0.05) in Figs. S6d-f represent the mean differences of vertical E-P flux significant at the 90% and 95% confidence levels, respectively. (g) Mean differences (grey pillars) and corresponding uncertainties (error bars) of Fz (area-weighted from 200 hPa to 10 hPa over 70°S-50°S) between sensitive experiments and the control experiment. The blue and red error bars reflect the 90% and 95% confidence levels calculated by two-tailed t test, respectively.

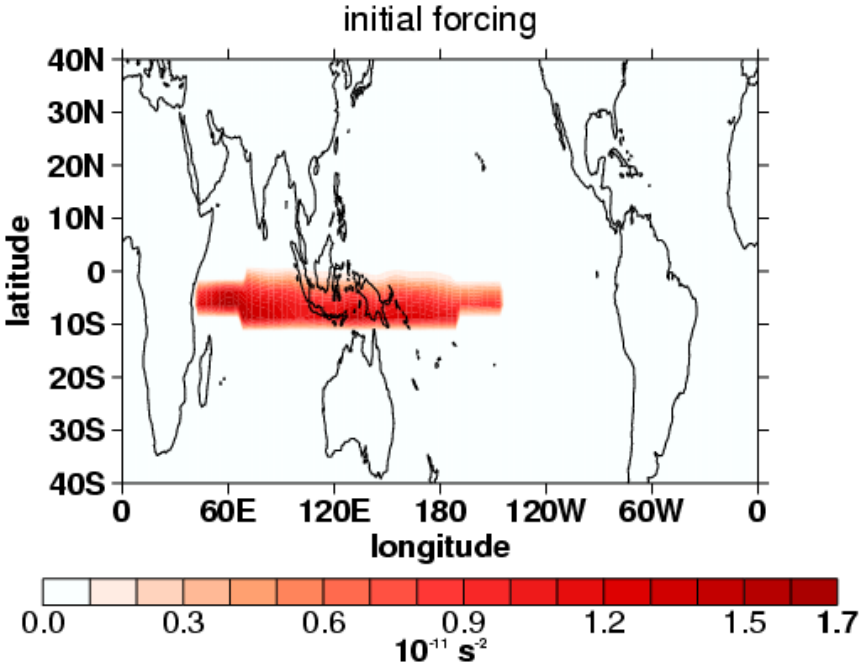

FIG. S7. The initial forcing ($R = -(f + \nabla^2\overline{\psi})D$) distribution in LBM.

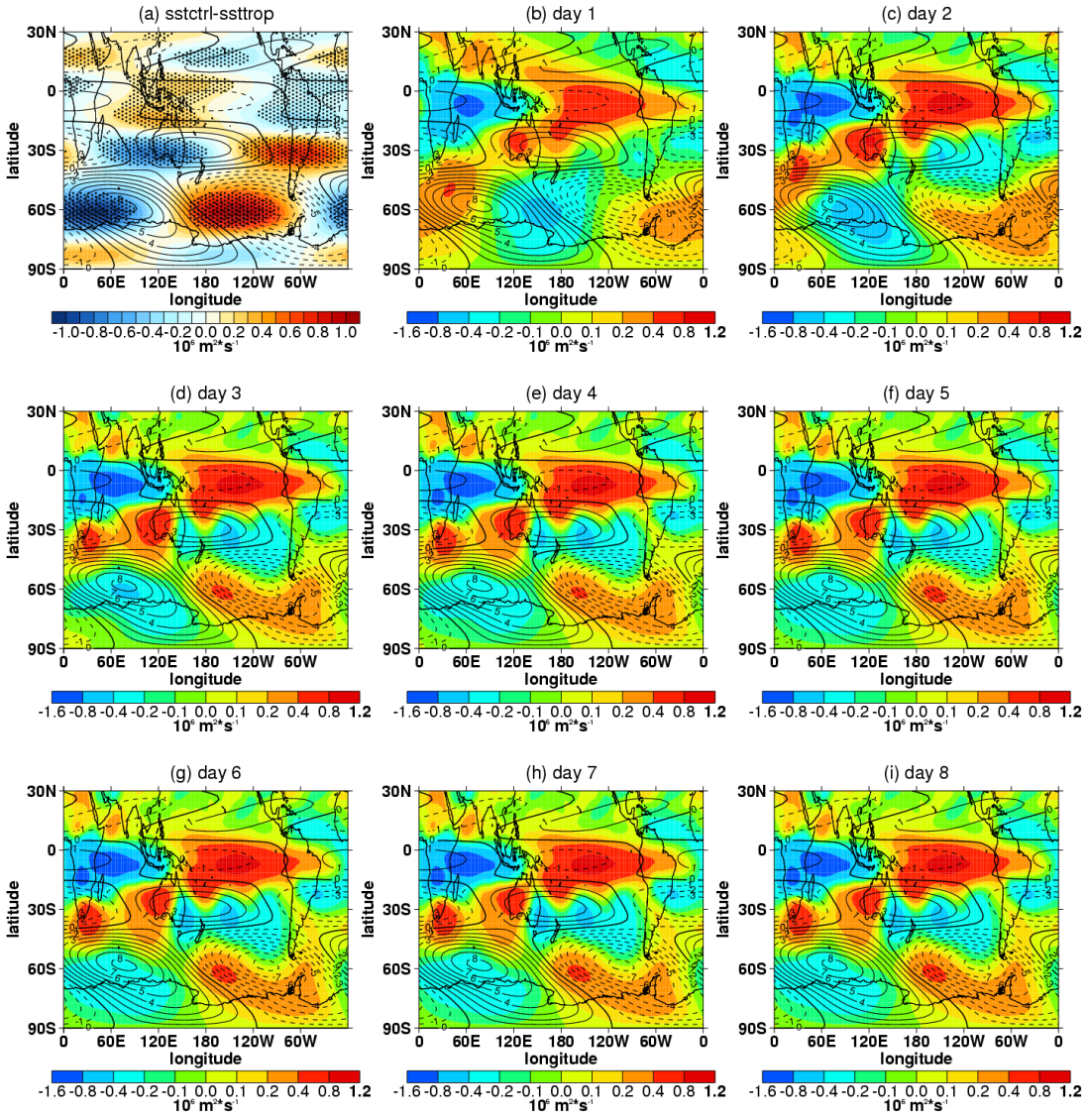

FIG. S8. The background field (contours with interval of 10^6 $m^2 \cdot s^{-1}$, positive and negative values are depicted by solid and dashed lines, respectively, zeros are depicted by thick solid lines) of streamfunctions derived from sstctrl and the responses (shadings) of streamfunctions derived from (a) ssttrop in CESM and (b-i) the first to eighth model days in LBM.

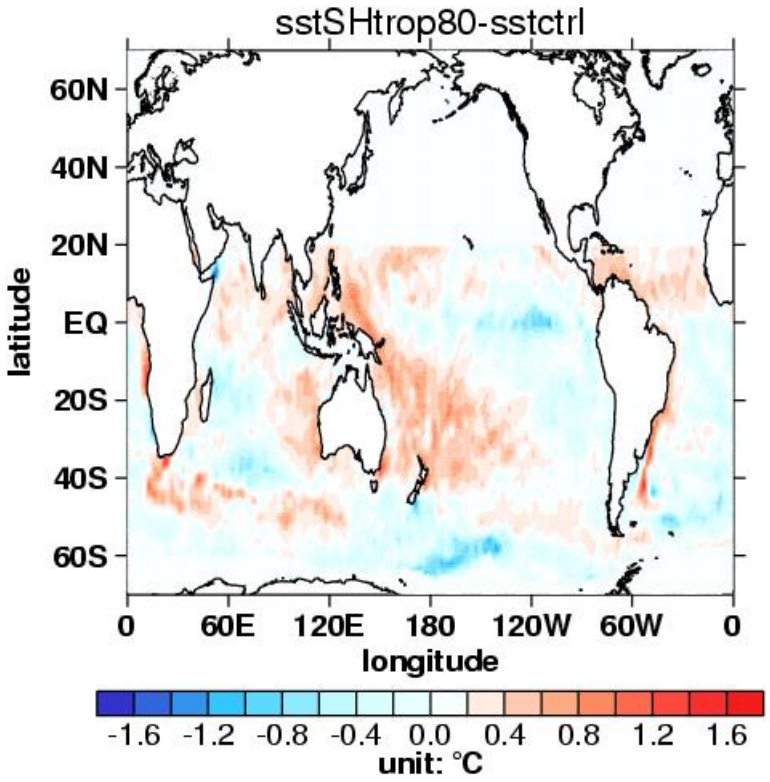

48

49 **FIG. S9.** Differences in SST forcing field between sstSHtrop80 and sstctrl.

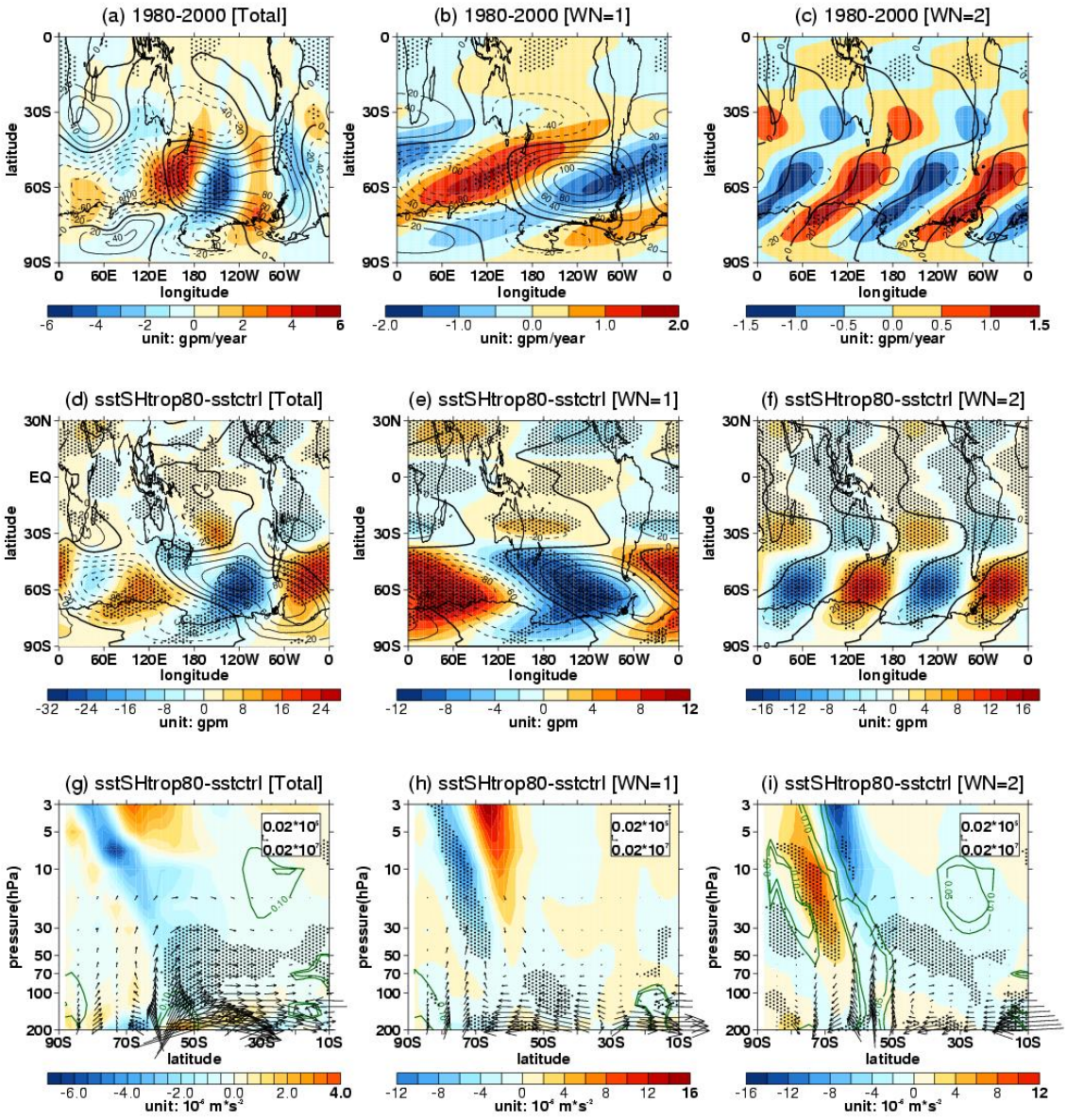

FIG. S10. (a-c) Trends (shadings) and climatological distributions (contours with an interval of 20 gpm, positive and negative values are depicted by solid and dashed lines respectively, zeros are depicted by thick solid lines) of southern hemisphere (a) 500 hPa geopotential height zonal deviation with their (b) wave-1 component and (f) wave-2 component in September during 1980-2000 derived from MERRA-2 dataset. (d-f) Differences (shadings) of (d) 500 hPa geopotential height zonal deviation with their (e) wave-1 component and (f) wave-2 component between sstSHtrop80 and sstctrl. The mean distributions (contours with an interval of 20 gpm, positive and negative values

are depicted by solid and dashed lines, respectively, zeros are depicted by thick solid lines) of the geopotential height zonal deviations are derived from sstctrl. (g-i) Differences of (g) stratospheric E-P flux (arrows, units in horizontal and vertical components are 0.02×10^{7} and 0.02×10^{5} $kg\cdot s^{-2}$, respectively) and its divergence (shadings) with their (h) wave-1 component and (i) wave-2 component between sstSHtrop80 and sstctrl. The stippled regions in Figs. S10a-f represent the trends or mean differences significant at/above 90% confidence level. The green contours from outside to inside in Figs. S10g-i represent the mean differences of vertical E-P flux significant at 90% and 95% confidence levels.

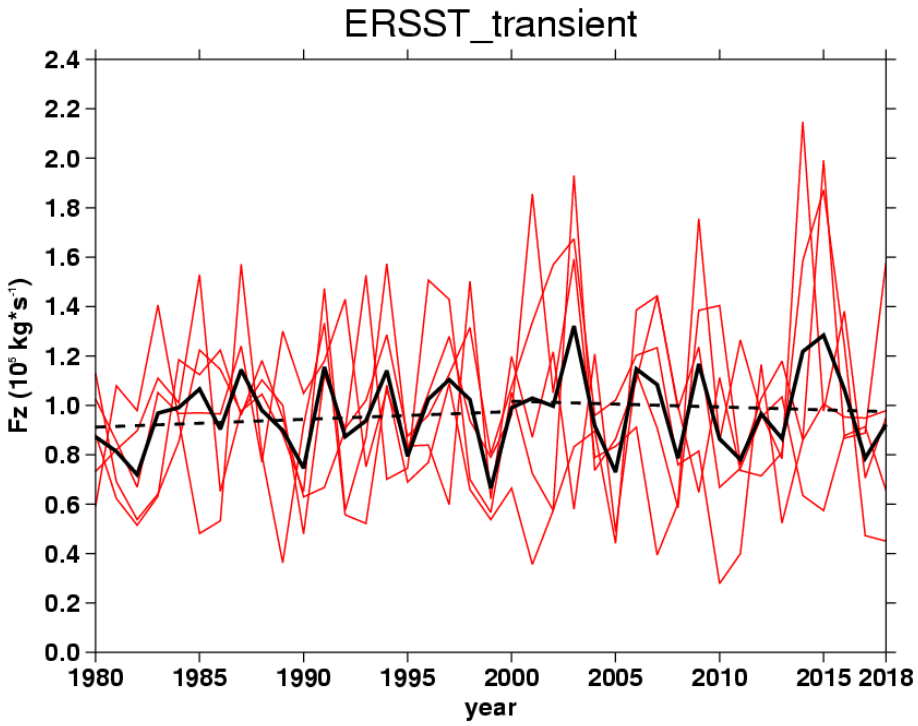

FIG. S11. Time series (solid lines) of vertical E-P flux area-weighted from 100 hPa to 30 hPa over 70°S-50°S in September during 1980-2018 derived from simulations forced by time-varying SST. Five different red solid lines stand for the time series driven by different initial conditions and the black solid line represent the ensemble

mean of them. The straight dashed lines show linear regressions to the ensemble mean on two piecewise period (1980-2000 and 2000-2018).

Table S1. Configurations of sstctrl, ssttrop and ssttropAug.

Experiments	Descriptions
sstctrl	Control run. Seasonal cycle of monthly mean global SST data over 1980-2000 is derived from the ERSST v5 dataset. Fixed values of ozone, greenhouse gases and aerosol fields in 2000 are used.
ssttrop	As in sstctrl, but with linear increments of SST in September over 2000-2017 superposed on the tropics (20°S-20°N). As shown in Figs. S4a-c, the global SST anomalies are applied from July to September.
ssttropAug	As in sstctrl, but with linear increments of SST in August over 2000-2017 superposed on the tropics (20°S-20°N). As shown in Figs. S4d-f, the SST anomalies are only applied from July to August.

Table S2. Trends of stratospheric vertical wave flux time series (averaged from 100 hPa to 30 hPa over 70°S-50°S) derived from different transient experiments (tr01, tr02, tr03, tr04, tr05) and ensemble mean of them on piecewise periods (1980-2000 and 2000-2018).

	tr01	tr02	tr03	tr04	tr05	ensemble mean
1980-2000	0.0091 (p=0.44)	-0.012 (p=0.32)	0.012 (p=0.15)	0.0031 (p=0.67)	0.0034 (p=0.77)	0.0031 (p=0.55)
2000-2018	-0.0060 (p=0.61)	0.0086 (p=0.67)	-0.030 (p=0.039)	-0.0034 (p=0.87)	0.019 (p=0.23)	-0.0023 (p=0.76)